

Numerical modeling of phase change phenomena during Drop/Wall interaction in the context of thermal spraying

Fathi Boukhazani^{1,2}, Redha Rebhi^{1,3}, Faouzi Didi⁴,  Ebrahim E. Elsayed^{5*}, Mohamed Kezrane^{1,2}

¹Department of Mechanical Engineering, Médéa University, Algeria.

²Laboratory of Mechanics, Physics and Mathematical Modelling (LMP2M), University of Medea, Algeria.

³Laboratory of Renewable Energies and Materials-LERM, University of Medea, Algeria.

⁴Department of Common Core in Technology, Laboratory of Physics of Experimental Techniques and Their Applications, University of Medea, 26000, Medea, Algeria.

⁵Department of Electronics and Communications Engineering, Faculty of Engineering, Mansoura University, Mansoura, 35516, Egypt; engebrahim16@std.mans.edu.eg (E.E.E.).

Abstract: In the thermal spraying process studied, a molten aluminum particle is projected at high speed and flattens upon impact with a substrate. This phenomenon is modeled and simulated thermomechanically using the explicit software Abaqus. Using this method, the study considers the three forms of heat transfer, which account for a variable thermal contact conductance, and the particle's and substrate's thermomechanical properties are considered temperature-dependent. The proposed model is first validated against both experimental observations and previously published numerical findings. Careful monitoring of the droplets' and substrate's temperature variations is maintained throughout the impact process. The starting velocity of the droplet, the substrate's temperature, and the substrate's material qualities are some of the variables that affect the thickness of the solidified layer that forms when the molten droplet contacts the substrate. By incorporating the combined thermal and mechanical interactions between the impacting particle and the substrate, the model also provides valuable insights into the processes of heat transfer and lamellae creation in thermal spraying.

Keywords: *Conductance, Heat transfer, Molten droplet, Solidification, Thermal spraying, Thermomechanical.*

1. Introduction

Thermal spraying plays a crucial role in surface treatment technology by applying a protective layer to enhance the characteristics of the target surface. This method surpasses other processes such as surface hardening, thermochemical treatments, or laser deposition. Its principle is based on heating particles until they melt, then accelerating them at high speed to bond them to the substrate or an existing coating. This process generates overlapping splashes to form a continuous coating layer, thus protecting against wear, corrosion, abrasion, erosion, and cavitation. After deposition, finishing operations are performed to achieve the desired dimensions, while treatments are applied to release residual thermal stresses, control porosity, and ensure coating homogeneity, thereby meeting usage criteria.

The choice of coating materials in thermal spraying is highly varied and largely depends on the desired performance. It includes a diverse range of materials such as metals (like copper, aluminum, tin, etc.), alloys such as stainless steels, bronzes, carbides (like tungsten carbide, nickel carbide, etc.), and even ceramics (like zirconia, titanium, chromium oxide, etc.). Target substrates can also be composed of different materials similar to those of the sprayed particles.

The diverse options available provide numerous industrial applications by minimizing the expenses linked to each coating selection. The microstructure of the deposits depends mainly on the cooling rate of the thermally sprayed droplets during and after solidification. The distribution of temperature within

the splats, as well as that of the substrate, determines the quality of the achieved cohesion. A wide range of thermal spraying methods has been designed to address different industrial requirements, each distinguished by factors such as operating temperature, particle velocity, coating material selection, and the level of thermal energy utilized. Frequently utilized methods encompass flame spraying, plasma spraying, cold spraying, wire arc spraying, detonation spraying, and high-velocity oxy-fuel (HVOF), among various others.

In thermal spraying, the outcomes of droplet/substrate interactions are influenced by numerous factors, which can be categorized into three main groups. Firstly, those related to the droplets include kinetic parameters, thermomechanical properties, phase transformations, particle sizes, particle shapes, etc. Secondly, factors associated with the substrate include surface condition, thermomechanical properties, heat transfer, initial temperature, phase transformations, presence of porosities, and a preliminary coating layer. Moreover, thirdly, those linked to the surrounding fluid, such as the nature of the fluid (gas type), flow type, etc. Additionally, the complexity of phase changes and the cooling of droplets, along with the heating/cooling of the substrate, further complicates the process, leading to a multitude of parameters affecting the phenomenon, making the study highly intricate.

Experimental results investigating the temperature variation of nickel droplets on different substrates have been conducted by Liu et al. [1]. During a recent study, it was evidenced that the thermal transfer coefficient underwent some impressive fluctuations before and after depositing nickel droplets on a metal substrate. The ability to do so is a result of the solidification of the nickel droplets on the specimen surface. Numerical simulation, in case of replication of these results, requires thus a non-constant transfer coefficient dependent on temperature. In the case of quartz surfaces, the change in this coefficient was quite small, which contributes to anchoring of the droplets and explains why quartz substrates are normally selected to be used in thermal sprays. The interaction between molten droplets and a cooler ground during thermal spraying was investigated in a study by Subedi and Kong [2] using the Smoothed Particle Hydrodynamics (SPH) approach. To further understand the droplet and substrate phase transitions, a solidification model was incorporated. By comparing these SPH results with experimental data recorded on different combinations of droplets and substrates, the method's validity was confirmed. The subsequent parametric study considered the impact velocity and the substrate properties and their effects on solidification. Based on the findings, cooling rates depend on the material of the substrate and the velocity of the droplet. However, they are always the same across all substrates regardless of their initial temperature. The work was further developed by Pasandideh-Fard et al. [3] who conducted experiments using molten tin droplets on a stainless-steel plate at varying substrate temperatures. They employed a modified SOLA-VOF approach to study the process, providing an opportunity to compare UCF predictions with experimental substrate temperature and the final diameter of the spreading droplets. The researchers could match the experimental results better by changing the thermal contact resistance, meaning that properly characterising contact resistance in modelling solidification behavior and droplet dynamics is fundamental. Attari et al. [4] used simulation, focusing on numerical modeling and prediction, to analytically study the consequences of flattening and deposition of aluminum particles. The temperature-dependent thermomechanical characteristics of the particles and the substrate used in their analysis were integrated into the Abaqus/finite-element system. Thermal conduction was estimated using a thermo-contact conductance that could be set. A comparison of the data obtained using the model and experimentally stored data described in previous studies is carried out. By tracking the change in temperature, displacement, Von-Mises stress, and equivalent plastic strain over time, the effects of particles may be evaluated. This method, which is driven by heat, sheds light on how lamellas form and heat is transferred during spraying, expanding our understanding of the mechanical interactions between particles and their substrates. An associated study was conducted by Aziz and Chandra [5] wherein parallel drops of molten tin were projected against a stainless steel surface in an experimental study. In order to calculate the thermal contact resistance at the interface between the droplets and the substrate, they compared the observed temperature changes to analytical solutions. Furthermore, the maximal spreading diameter was predicted using a simplified

energy conservation model, which thereby confirmed the results. Similarly, Trapaga et al. [6] explored the influence of molten particles, reporting that large droplets ($\sim 5\text{mm}$) striking metallic substrates at velocities near 2 m/s produced distinct impact effects. Additionally, a 2D numerical model was created to mimic the actions of smaller particles ($\sim 100\mu\text{m}$) colliding at substantially greater velocities, approximately 100 m/s . According to their findings, larger droplets undergo both solidification and spreading simultaneously, whereas smaller ones undergo spreading first. The reason behind this variation is that when droplet velocities are low, the dominant force is kinetic energy, and the spreading process occurs on a very short time scale. As a result, the temperature of the molten droplet does not cool down much, which delays solidification. Smaller droplets were expected to cool more quickly than larger ones. The study did not consider substrate melting and solidification. As part of their research on welding deposition, Attinger et al. [7] used tiny droplets whose diameters varied between 50 and $100\ \mu\text{m}$. They tested different substrate temperatures to determine the propagation of droplets, deposition factor, dimensionless splash height, and solidification time. In contrast to the real speed of the thermal spraying process, the droplet velocity was low, at around 2 m/s . Because of this, the spreading and solidification processes were slowed down. The effects of liquid tin droplets on sapphire surfaces were studied by Gielen et al. [8] at different temperatures, and they used scaling arguments to quantify the spreading of the droplets and the formation of ligaments through splash. In their presentation, the authors used the Weber and Stéphan numbers to illustrate three impact behaviors: splash, deposition, and rebound. Zhang et al. [9] investigated splash morphology as well as substrate fusion and regeneration during the solidification of molybdenum droplets impacting glass, mild steel, and molybdenum surfaces, combining both numerical simulations and experimental observations. They monitored the change of the interface between the droplets and the substrate by using a 1D solidification framework and the Volume of Fluid (VOF) technique. According to their parametric study, the amount of substrate fusion and recrystallization is greatly affected by variables including substrate temperature, droplet impact temperature, and the thermophysical characteristics of both materials.

Dalir et al. [10] examined the SPS process using a 3D unsteady magnetohydrodynamic model. The researchers used an Eulerian-Lagrangian approach. Researchers in this study looked at how Yttria-Stabilized Zirconia (YSZ) and other droplet shapes affected the SPS procedure. Because of the uneven pressure forces, droplets deform, changing their drag coefficient. The study accurately simulates droplet atomization using the KHRT rupture model and a dynamic drag law. Implementing the dynamic drag law significantly reduces the proportion of melted particles, according to the results. Moreover, a higher solid concentration leads to a denser coating due to melted particles landing at higher speeds. Zeoli et al. [11] studied a numerical model that integrates the cooling and fragmentation of metal droplets during atomization in an electricity production process. This model, simulating interactions between droplets and the gas flow, reveals that the initial droplet size strongly influences their thermal history. The findings prove that big droplets avoid undercooling, but tiny ones go through three separate processes: undercooling, clarification, and recalescence.

Furthermore, the forecasts show that droplet shapes remain consistent when gas is atomized and that the in-flight distance dictates how droplets solidify and atomize. Grant et al. [12] developed a computational framework to analyze the thermal and dynamic behavior of atomized gas droplets during spray formation. In one recent study, a multidisciplinary model has been developed that encompasses droplet cooling, solidification, and droplet-gas interactions together, simplifying therefore to determine the droplet size, gas velocity, and novel melt composition as the dominant factors. Sprayed solid fraction, a parameter to refine predictions of surface temperature and solidification behavior, was estimated using empirical distributions of droplet sizes and gas-velocity measurements. Alavi and Passandideh-Fard [13] explained the effect of thermal contraction when conducting thermal spraying; the authors considered the deposition of molten tin droplets on a steel surface. They modelled the variation of density induced by solidification and cooling with the help of the Volume of Fluid (VOF) method. Their models were carried out using both in-house developed programmes and commercial codes (FLUENT), with different velocities of the spherical tin droplet imposed. The findings

demonstrated that upon impact, droplets disperse and solidify, creating a single cavity upon recoil, which causes porosity in the splat due to thermal contraction. A splat with an irregular shape was modeled for cooling and solidification using the network simulation method by Sánchez-Pérez et al. [14]. Numerical simulations with high performance are achieved by using optimized circuit analysis algorithms and finite difference methods to incorporate and evaluate specific thermal process conditions accurately. The splat's geometry is derived from experimental data obtained through electron microscopy.

Additionally, the model considers both phase change phenomena and material property variability with temperature. Physical behavior analysis utilizes nondimensionalization, aiding in the interpretation of simulation results. Notable results include the development of columns and horizontal bars that preserve the splat structure as the material solidifies. Furthermore, the investigation yields two monomials: one that associates radiation with conduction (similar to the Nusselt number in its application to convection) and the other that associates solidification time with the Stefan number.

By modelling the effects of various operational circumstances on the deposition of particles in cold spray, Xie et al. [15] examined the effects of high-velocity collisions of spherical particles on a flat substrate. To address the challenges of extreme deformation, they proposed a Coupled Euler–Lagrange (CEL) numerical approach, which highlighted the presence of a compressive stress zone generated by intense plastic deformation at the particle–substrate interface. Owing to the short contact duration and high pressures, this deformation remained localized at the base regions of both the particle and the substrate. Investigation determines that the efficiency of deposition greatly relies on the original particle temperature, the velocity of impact, the frictional characteristics, and the material combination. High-density materials, in particular copper, were discovered to provide better interfacial bonding due to high kinetic energy at impact. The results indicate that the CEL method offers higher robustness and stronger accuracy for modeling high-speed deformation processes compared to other accessible methods.

In a parallel study, Xue et al. [16] utilized a model to assess the thermal characteristics of interactions between liquid and solid substrates by collecting data on contact pressure, surface roughness, and the effective area of actual contact between molten metal and solid surfaces. Researchers calculated the thermal contact resistance and its time-dependent variation by including a time-dependent computational method of three-dimensional free-surface flow and heat transfer. After that, the model was employed to analyze how the droplet spread, solidified, and was impacted by other objects, all while providing distributions of the thermal contact resistance at the interface between the liquid and solid. The tests included nickel particles ($\sim 50\ \mu\text{m}$) bombarded with plasma and allowed to accumulate on steel surfaces, as well as molten aluminum alloy droplets ($\sim 4\ \text{mm}$) on solid samples. Modeled splash-shaped morphologies were compared to experimental images, and modeled temperature time evolutions at impacts were compared to measured values.

Liao et al. [17] studied the solidification and melting of zirconia splats through the application of a three-dimensional computational model. The thermal contact resistance was explicitly considered at the droplet/substrate interface in their computational fluid dynamics (CFD) research. Experimental outcomes indicated that maximum substrate melting can only be achieved under the condition of smooth surfaces with negligible thermal resistance and disk-like splats deposited. In comparison, when the thermal contact resistance is finite, high-velocity solidification at the splat boundaries forms a central splash surrounded by non-drop droplets. Suli et al. [18] then studied the maximum spreading factor achievable by molten droplets that strike and solidify on the metal surfaces. A systematic investigation was conducted to examine the effects of substrate temperature, specific heat capacity, impact velocity, thermal conductivity, and droplet size. A Volume of Fluid (VOF) technique was employed to monitor the droplet's free surface. The use of convection and phase-change phenomena was included by embedding the model into the energy and Navier-Stokes equations; along with these equations, the Level Set function was used to keep track of the air-molten boundary. An organized study of the comparison of propagation factors with published experimental information has been carried out.

To this effect, Danouni et al. [19] initiated an exploratory study that sought to develop a simulation model that could quantify the transient interaction a particle had with a substrate. The authors also examined the merits of coupled heat-transfer and structural-behavior equations to characterize temporal changes to properties. These were executed using the Ansys software through the direct coupling approach. The structural model was determined first without considering the effects of heat transfer. Thermoelastic effects were then ignored, and thermomechanical coupling was introduced, after which a further set of simulations was conducted, taking into account thermal-elastic coupling. The quantitative findings make obvious the extremely significant role of thermal factors in contact problems and illustrate the impossibility of an effective description of the structural and thermal behavior without the introduction of elasticity. Together with Zhao et al. [20], the suspension plasma spray technique was used to deposit YSZ on several substrates, including aluminium and stainless steel. They investigated substrate properties that included material, surface topology, temperature, and coating thickness. Coatings applied to aluminum had greater porosity than those applied to stainless steel under the same spraying conditions, presumably because aluminum has a better thermal transfer capacity than stainless steel. Scanning electron microscopy revealed that adjusting the formation mechanism and enhancing substrate surface roughness can alter the coating microstructure from a vertically cracked pattern to a columnar arrangement. It was discovered that the microstructural characteristics in the interface region were more affected by the substrate's preheating temperature. Improving coating adhesion and decreasing interface defects can be achieved by raising the substrate temperature. The coatings' vertical cracks become narrower and fewer in number as the substrate thickness increases. Premaram et al. [21] examined the development of wear-resistant coatings on aluminum and magnesium engine block cylinders, as well as cylinder bores, aiming to enhance corrosion and abrasion resistance. The use of nanocomposite coatings, applied via plasma spraying, enhances tribological properties and prevents wear and cracking mechanisms. Tang et al. [22] prepared embedded micro-agglomerated particle (EMAP) coatings by spraying two kinds of powders simultaneously using the atmospheric plasma spraying technique. To examine how the spraying angle affected particle deposition and coating performance, four different angles were used, spanning from 90° to 30°. Spraying at a lower angle results in a lower relative deposition efficiency, harder coatings, and a lower elastic modulus, according to the experiments. As the spraying angle drops from 90° to 50°, porosity decreases, but it spikes significantly at 30°. The coating contains the highest percentage of second-phase particles, 10.8%, when sprayed at a 90-degree angle. The relative quantity is 2.2% at a spraying angle of 30°, which is the lowest amount currently observed. In addition, at small angles, the first-phase matrix powder's molten droplets extend and break apart along the angular direction. At a spraying angle of 90°, the most stable thermal shock life was achieved, with a maximum average of 40.6 cycles. Thermal shock life and stability were both negatively affected by reducing the spraying angle. Zirari et al. [23] examined how an aluminum particle, whether completely or partially molten, impacts an H13 tool steel substrate. Subsequently, it was investigated how the angle of the particle affected a flat surface following its partial melting. Splat morphologies are significantly affected by the particle's melting state, according to their findings.

Pasandideh-Fard and Mostaghimi [24] have studied the mechanical forces experienced by a liquid droplet when it spreads itself on a thermally contact-resistant surface and solidifies. In their study, they concentrated on the role of solidification on the growth of droplets, and they pointed out the role of the thermal contact resistance in such a system. Analysis used a modified SOLA-VOF method to solve the full Navier-Stokes equations on an axisymmetric rectangular grid, and droplet solidification was a one-dimensional heat-conduction model. The obtained results showed that even the last splat diameter significantly relies on the given thermal contact resistance level. That solidification was disclosed to show an intense effect with the rise in the Reynolds and Stefan numbers.

Having gained knowledge in previous research studies, Oukach et al. [25] investigated the behavior of molten droplets on stiff substrates at the millimeter scale with fluid flow, heat conduction, and phase transition. Their findings show that the initial temperature of the droplet and the material used in the

substrate will play a significant role in the duration of solidification and spreading behavior, as well as contact thermal resistance being a key factor. The air-droplet interface was captured by a numerical model that couples the energy and Navier-Stokes equations with a Level Set function, and the simulation was carried out with the Finite Element Method in Comsol Multiphysics 3.5a.

The present numerical work further explores the solidification of molten aluminum droplets in thermal spraying, examining how factors such as substrate initial temperature, particle velocity, substrate composition, and particle concentration influence splat formation across different substrate grades. The research focuses on evaluating a simulation method for the impact and solidification process using a thermomechanical model. This model accounts for temperature-dependent material properties, incorporates the different modes of heat transfer, and applies a correlation for variable thermal contact conductance. The governing equations are solved using Abaqus/Explicit software.

2. Physical Model and Mathematical Formulation

Thermal spraying is carried out by propelling molten particles toward a substrate using a controlled spray gun. As depicted in Figure 1, an optimal coating layer is achieved when particles of varying sizes and geometries strike the target surface at different velocities and incidence angles. To simplify the analysis of this complex process, the effect of a single droplet impacting the substrate is considered. In the present study, attention is placed on the normal impact of a spherical molten droplet, as shown in Figure 1, where D denotes the initial droplet diameter, $T_{droplet}$ its initial temperature, U the impact velocity, and T_w the substrate's initial temperature.

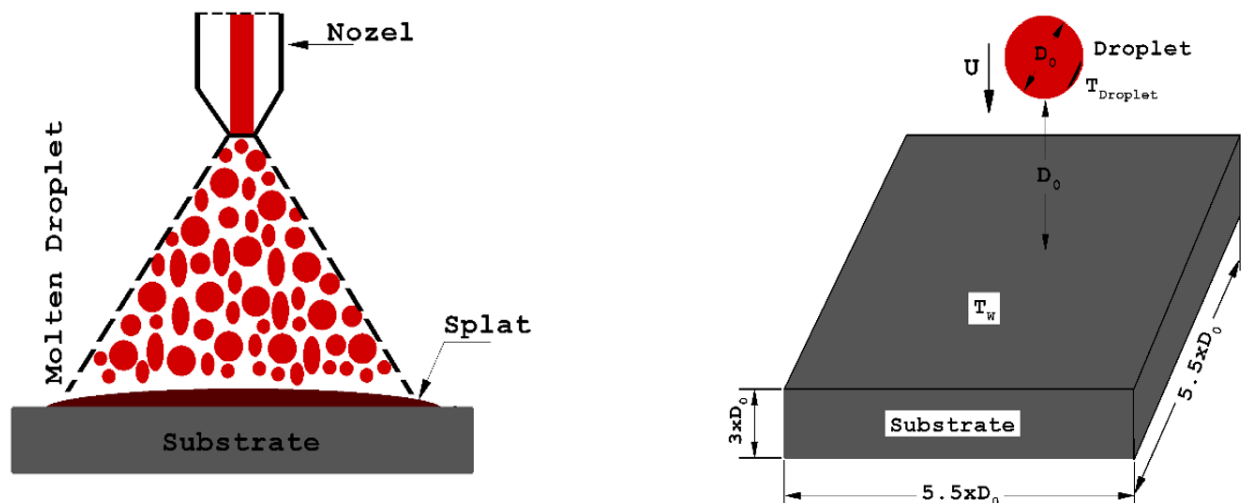


Figure 1.
Thermal spray processes and physical model under analysis.

The governing heat transfer equations are solved in ABAQUS/Explicit using an explicit forward-difference time integration scheme [4]. The temperature at a node N for increment $i + 1$ is expressed as:

$$\theta_{(i+1)}^N = \theta_{(i)}^N + \Delta t_{i+1} \dot{\theta}_{(i)}^N \quad (1)$$

where θ^N is the nodal temperature and i represents the increment index in a dynamic step. The initial temperature rates are obtained from:

$$\dot{\theta}_{(i)}^N = (C^{NJ})^{-1} (P_{(i)}^J - F_i^J) \quad (2)$$

Here, F^J is the internal flux vector, C^{NJ} is the lumped capacitance matrix, and P^J denotes the applied nodal source vector. The capacitance matrix is defined as:

$$[C] = \int_0^V [V]^T \rho \left(\frac{\partial H}{\partial T} \right)^t N dV \quad (3)$$

Within the solidification region, the specific heat capacity is expressed as:

$$C_p(T) = \frac{\partial H}{\partial T} - \frac{H_f}{(T_{liq} - T_{sol})} \quad (4)$$

where H_f is the latent heat of fusion, while T_{sol} and T_{liq} are the solidus and liquidus temperatures, respectively.

The motion equations of the body are integrated explicitly using the central-difference method:

$$\dot{\mu}_{(i+1)}^N = \dot{\mu}_{(i-\frac{1}{2})}^N + \frac{\Delta t_{i+1} - \Delta t}{2} \ddot{\mu}_{(i)}^N \quad (5)$$

$$\mu_{(i+1)}^N = \mu_i^N + \Delta t_{i+1} \dot{\mu}_{(i+\frac{1}{2})}^N \quad (6)$$

where μ^N is a degree of freedom (displacement or rotation); the central-difference operator updates the kinematic state explicitly using known velocity and acceleration values from the preceding increment.

The material response is assumed to be linearly elastic, described by the Mie-Grüneisen equation of state. In ABAQUS, pressure is expressed as:

$$P - P_H = \Gamma_\rho (E_m - E_H) \quad (7)$$

with Γ^F representing the Grüneisen ratio, and P_H and E_H being Hugoniot pressure and energy, which depend on density. The ratio is defined as:

$$\Gamma = \Gamma_0 \frac{\rho_0}{\rho} \quad (8)$$

Where Γ_0 and ρ_0 are material constants. Hugoniot energy is given by:

$$E_H = \frac{P_H \eta}{2\rho_0} \quad (9)$$

with $\eta = 1 - \frac{\rho_0}{\rho}$, representing nominal compressive strain. Substituting into previous relations yields:

$$P = P_H \left(1 - \frac{\Gamma_0 \eta}{2} \right) + \Gamma_0 \rho_0 E_m \quad (10)$$

Hugoniot data are typically fitted using:

$$P_H = \frac{\rho_0 c_0^2 \eta}{(1-s\eta)^2} \quad (11)$$

where c_0 and s describe the linear relation between shock velocity U_s and particle velocity U_p :

$$U_s = c_0 + sU_p \quad (12)$$

Hence, the Hugoniot form becomes:

$$P = \frac{\rho_0 c_0^2 \eta}{(1-s\eta)^2} \left(1 - \frac{\Gamma_0 \eta}{2} \right) + \Gamma_0 \rho_0 E_m \quad (13)$$

At minor compressive strains, the bulk modulus reduces to $\rho_0 c_0^2$.

Viscosity evolution is described by the Arrhenius relationship [26]:

$$\mu(T) = \mu_0 \exp\left(\frac{E}{RT}\right) \quad (14)$$

where μ_0 is the pre-exponential factor, E the activation energy for viscous flow, T the absolute temperature, and R the universal gas constant ($8.3144 \text{ J} \cdot \text{mol}^{-1} \cdot \text{K}^{-1}$).

3. Numerical Simulation

In this study, due to the presence of significant deformations accompanied by simultaneous heat exchange, a coupled temperature-displacement dynamic approach was adopted. Mapped triangular meshing was applied to the bounding faces where appropriate. The element type selected for modeling both the particle and the substrate is C3D10MT, a second-order 10-node tetrahedral element, thermally modified and equipped with hourglass control, well-suited for complex thermo-mechanical analyses. A quadratic bulk viscosity was also introduced to enhance numerical stability. To ensure realistic

interactions at the interface, a surface-to-surface contact algorithm was applied, with the coefficient of friction assumed to remain constant and independent of temperature throughout the simulation. In this work, an aluminum particle is modeled impacting three different metallic substrates: nickel, stainless steel, and copper, using the Abaqus/Explicit solver. The particle is initialized at a temperature of 660 °C and a velocity of 150 m/s, while the substrate temperature ranges between 20 °C and 100 °C.

As shown in Figure 2, the mesh density has an apparent effect on the accuracy of the results. Simulations conducted with a coarse mesh (5724 nodes) exhibit larger deviations and scattered trends, whereas the semi-fine mesh (11,448 nodes) yields predictions closer to experimental data. The fine mesh (17,172 nodes) achieves the best agreement, with minimal error. Consequently, all subsequent numerical simulations in this study adopt the fine mesh configuration to ensure higher accuracy.

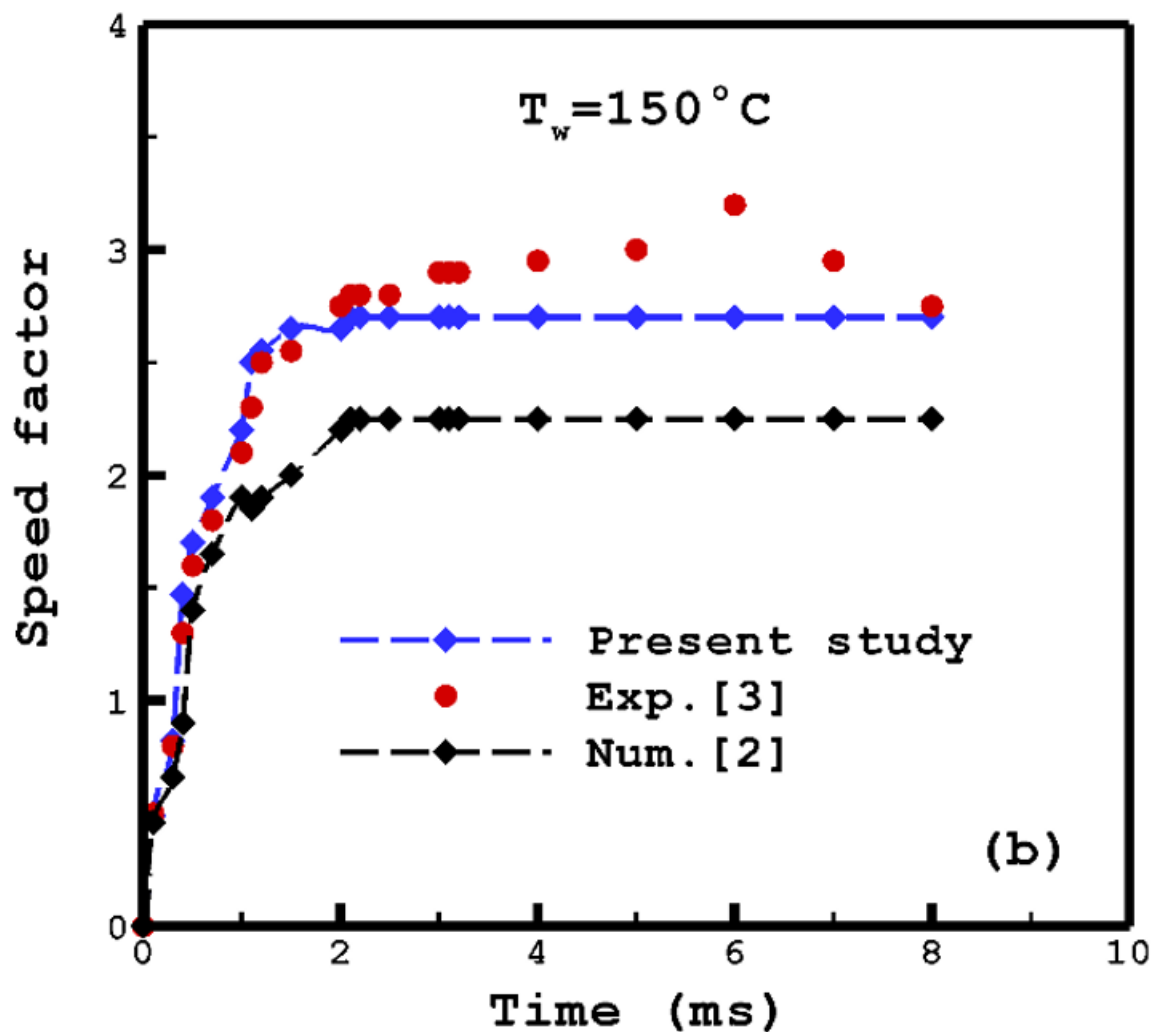


Figure 2.
Magnetization Grid of Sensitivity of Mesh.

This study begins by examining the normal impact of a molten tin droplet on a flat stainless-steel substrate, confirming earlier experimental results reported by Pasandideh-Fard et al. [3] and numerical simulations conducted by Subedi and Kong [2] using the SPH method. Figure 3 presents our

experimental observations for wall temperatures of 25°C and 150°C, where a 2.1 mm diameter droplet impacted the substrate at a velocity of 1.6 m/s under both thermal conditions ($T_w = 25\text{ °C}$ and 150 °C). In each case, the droplet temperature was initialized at 240 °C, slightly above its melting point of 232 °C, consistent with both computational and experimental findings.

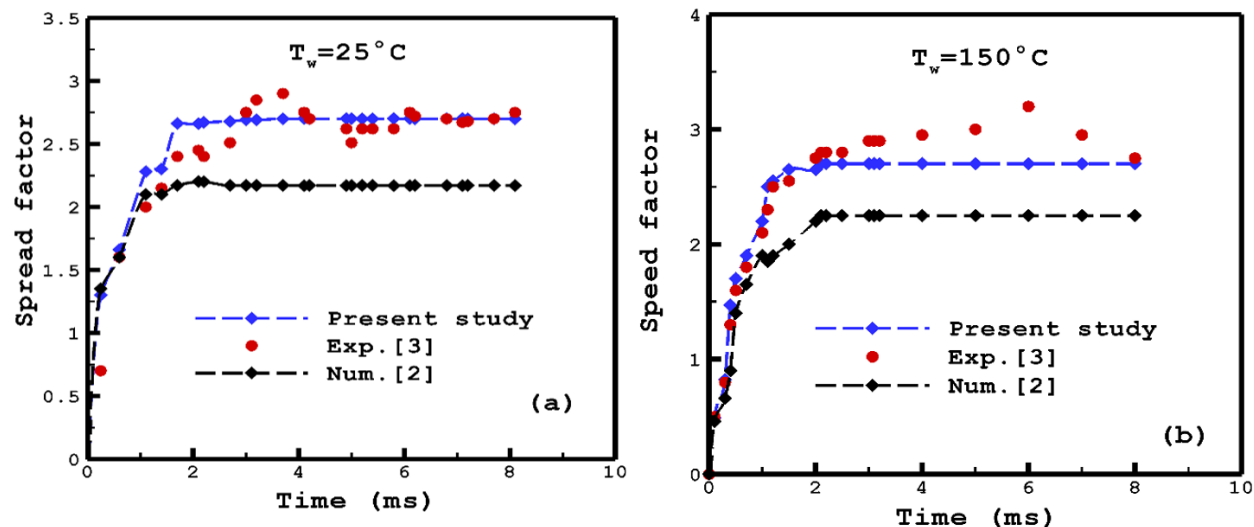


Figure 3. A tin droplet's spread factor changes at (a) $T_w = 25\text{ °C}$ and (b) $T_w = 150\text{ °C}$ on a stainless-steel substrate.

As shown in Figure 4, we examined the effect of 25°C and 150°C wall temperatures on a stainless-steel substrate of a molten tin droplet. In both temperature conditions, the 2.1 mm diameter droplet moving at 1.6 ms^{-1} was employed. An initial temperature of 240°C, slightly above its melting point of 232°C, is suggested by results from both experiments and computer models. It successfully depicts the spread factor's trend. The results are in agreement with simulation measurements, even though both experimental data and simulations have limitations. In both scenarios, the rate of spreading is precisely recorded up to approximately 2 ms, indicating that the droplets spread during impact. As the molten droplet solidifies, the numerical results begin to differ slightly from the experimental data after 2 ms, and the spread factor takes on a constant value. The current study incorporates the mushy zone simulation. The solidification model states that when liquid particles solidify, they are given the properties of infinity in terms of viscosity (no spreading) and zero velocity. This property stops the droplet from spreading any further. Tin in its molten state oxidizes quickly in the presence of air. A few oxide layers form on the droplet as it travels through the air prior to impact and spreading because of its rapid cooling and considerable deformation. A polished stainless-steel specimen was also used in this experiment. Although surface roughness slows solidification and heat transfer, it also makes it harder for droplets to spread. Therefore, the present models take surface roughness into account.

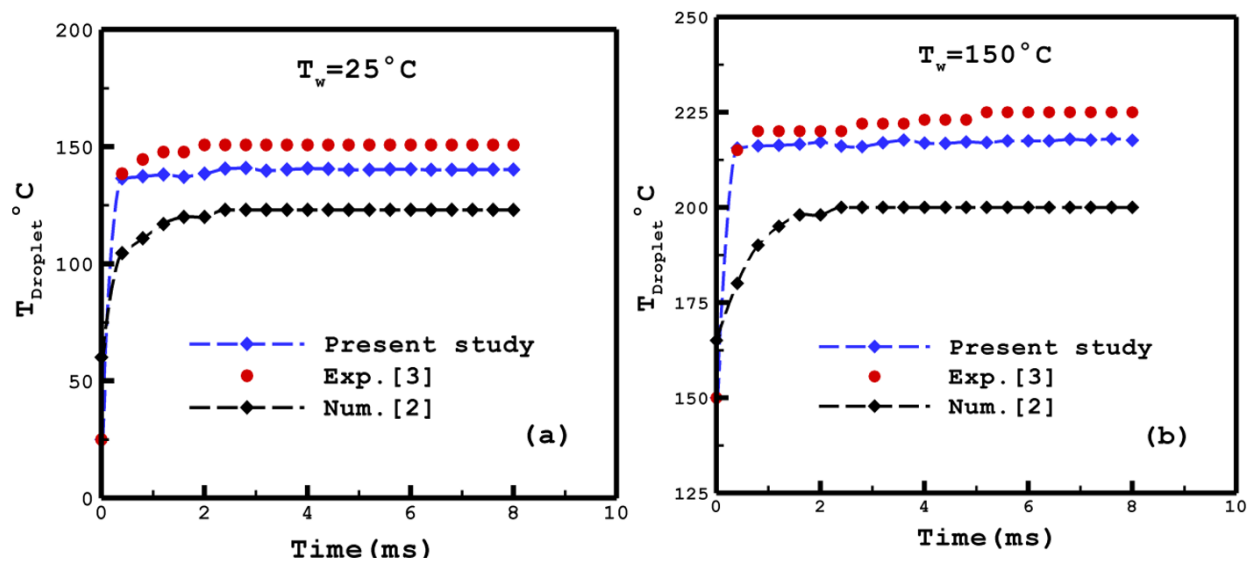


Figure 4. Temperature evolution at the impact point of a tin droplet on a stainless-steel substrate at two initial wall temperatures: (a) $T_w = 25\text{ }^\circ\text{C}$ and (b) $T_w = 150\text{ }^\circ\text{C}$.

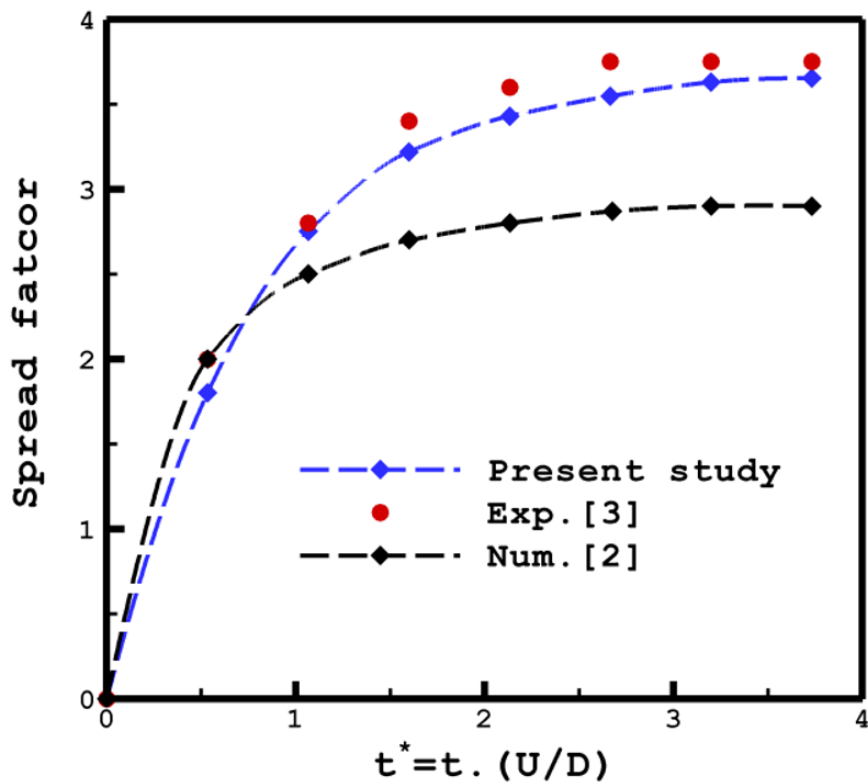


Figure 5. Evolution of the spread factor for a tin droplet impacting an aluminum substrate (substrate temperature $T_w = 25\text{ }^\circ\text{C}$, droplet temperature $T_D = 267\text{ }^\circ\text{C}$, droplet diameter $D = 3.7\text{ mm}$, and impact velocity $U = 2.48\text{ m/s}$).

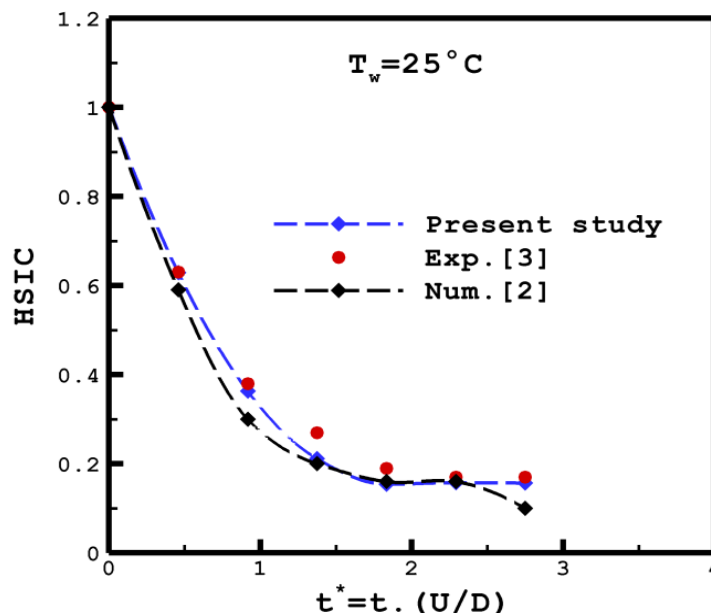


Figure 6.

Evolution of the dimensionless central splat height for the high-speed impact and contact (HSIC) of a copper droplet on a copper substrate. The simulation parameters are: droplet temperature ($T_D = 1531$ K), substrate temperature ($T_w = 295$ K), impact velocity ($U = 2.52$ m·s⁻¹), and droplet diameter ($D = 4.67$ mm).

The numerical model accurately depicted the rapid increase in substrate temperature following impact, as measured at the center of the impact. According to the results of the experiments, the temperature remains relatively constant after a very rapid initial rise. However, the present simulations show a steady rise towards a steady-state temperature.

Trapaga et al. [6] for the dimensionless splat height of copper (Cu) droplets striking a copper (Cu) substrate and the dimensionless spread factor of tin (Sn) droplets striking an aluminum (Al) substrate, these were also compared to this model. This allowed us to assess the impact of different substrates and droplet materials.

The simulation considered a case in which a tin droplet, 3.7 mm in diameter and initially at 267°C, impacted an aluminum substrate maintained at 26°C. The droplet approached vertically with a velocity of 2.48 m·s⁻¹. In a similar vein, when considering copper on copper, the model represented a molten droplet that started at 1252°C, had a diameter of 4.67 mm, and was moving vertically at a velocity of 2.52 m·s⁻¹, striking a substrate at 22°C. In Figures 5 and 6, corresponding assessments are shown. Since the model considers thermal conductivity, the spread factor agrees with the experimental data.

Other thermal spray phenomena, such as the droplet's melting and re-solidification, and temperature distribution, will be studied using the model in the paper's later sections.

4. Results and Discussion

In order to gain a better understanding of the droplet solidification phenomenon within the thermal spraying process, two case studies were conducted: the first focused on a single particle, while the second involved a multiparticle configuration.

4.1 A Single Particle

The numerical model developed in this study simulates the impact and spreading of a single aluminum particle on a steel substrate during thermal spraying, employing an explicit dynamic

formulation that couples temperature and displacement. The first stage of this work focuses on validating the model by comparing its predictions with previously reported results. For example, Subedi and Kong [2] investigated a similar problem using the SPH method. At the same time, Liu et al. [1] reported observations that closely resemble the early contact behavior captured in our simulations (Figures 7 and 8). Differences in methodology account for variations in particle flattening and spreading factors across the studies.

Our results illustrate the thermal evolution of a 2.1 mm diameter tin droplet impacting a stainless-steel surface at two substrate temperatures (25 °C and 150 °C). The droplet enters with an initial velocity of 1.6 m/s and a temperature of 240 °C, slightly above its melting point. Upon impact, it undergoes spreading and progressive solidification. As demonstrated in Figures 7 and 8, the substrate's initial temperature plays a crucial role in governing the cooling rate of the metal, thereby affecting the droplet's solidification dynamics over time. Figure 9, which displays the droplet contours at various time intervals, provides additional support for this observation. Additionally, the commencement of solidification is evident upon the droplet's contact with the substrate. The reason for this is that the droplet undergoes a phase transition from liquid to mushy, and subsequently to solid, as the kinetic and thermal energy dissipate simultaneously.

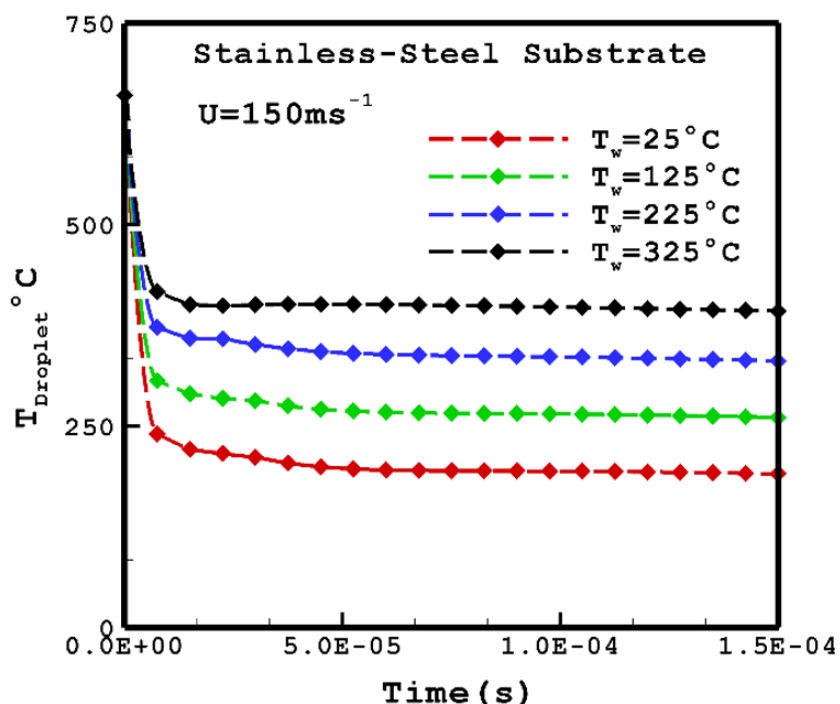


Figure 7. Thermal response of an aluminum droplet impacting a stainless-steel substrate at varying wall temperatures ($U = 150 \text{ ms}^{-1}$).

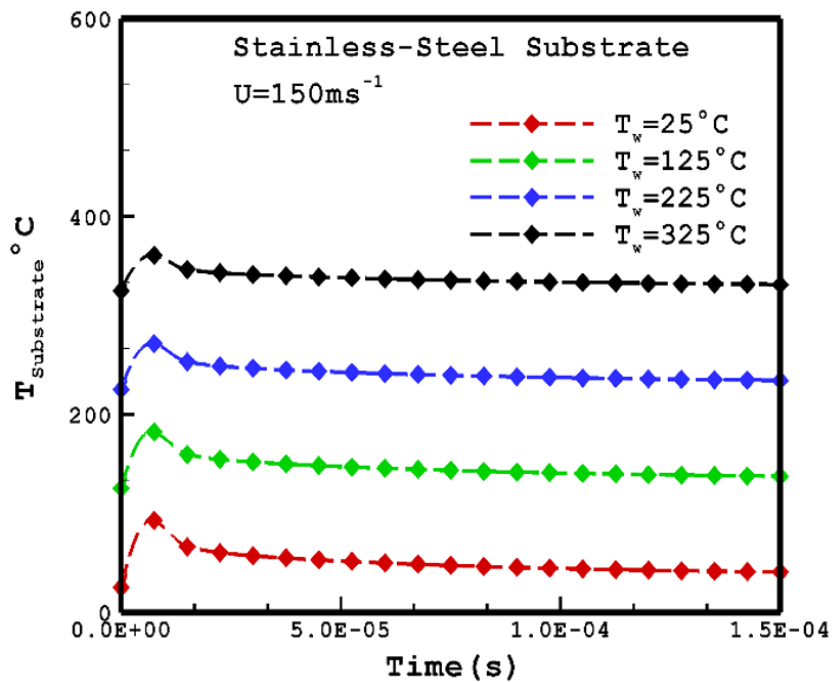


Figure 8. Transient temperature evolution at the impact point of a stainless-steel substrate by an Aluminum droplet at various initial substrate temperatures ($U = 150\text{ms}^{-1}$).

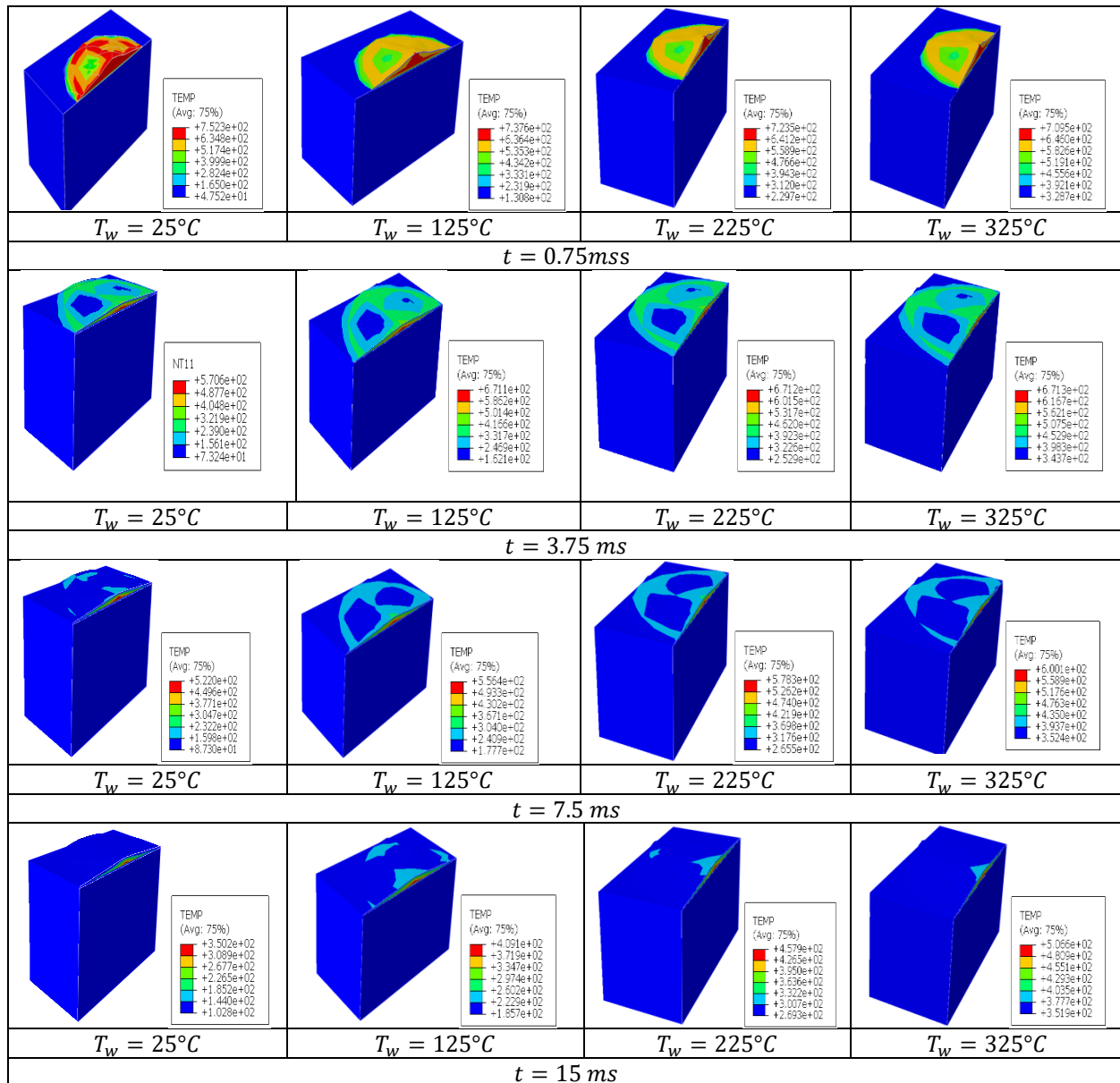


Figure 9. Temperature contour distribution for varying substrate temperatures.

The spreading behavior of droplets is strongly dependent on their impact velocity, as shown in Figure 10. Higher velocities lead to greater deformation, which enlarges the contact area with the substrate and thereby enhances the heat transfer rate. This relationship is further confirmed by the observed link between impact speed and the thickness of the solidified layer, as demonstrated in Figures 11 and 12.

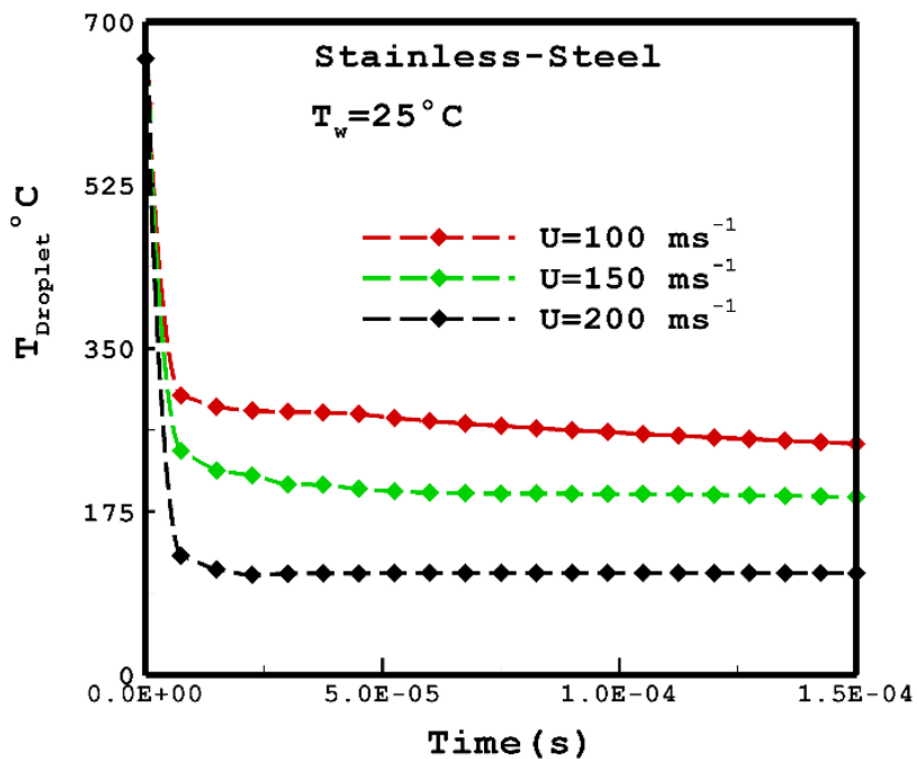


Figure 10. Temporal evolution of the temperature of an aluminum droplet subjected to various impact velocities on a Stainless-Steel Substrate, $T_w = 25^\circ\text{C}$.

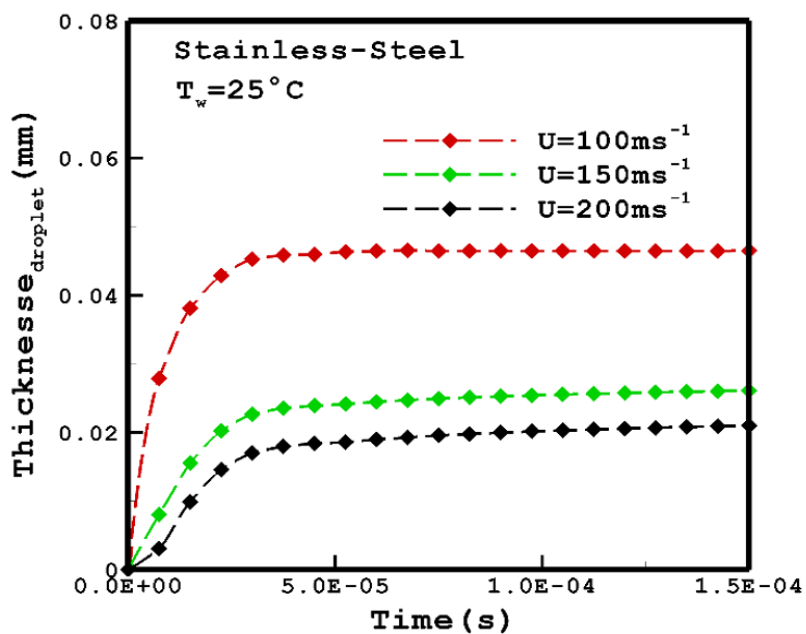


Figure 11. Temporal evolution of the solidified layer thickness of an Aluminum droplet impacting a stainless-steel substrate at different velocities, $T_w = 25^\circ\text{C}$.

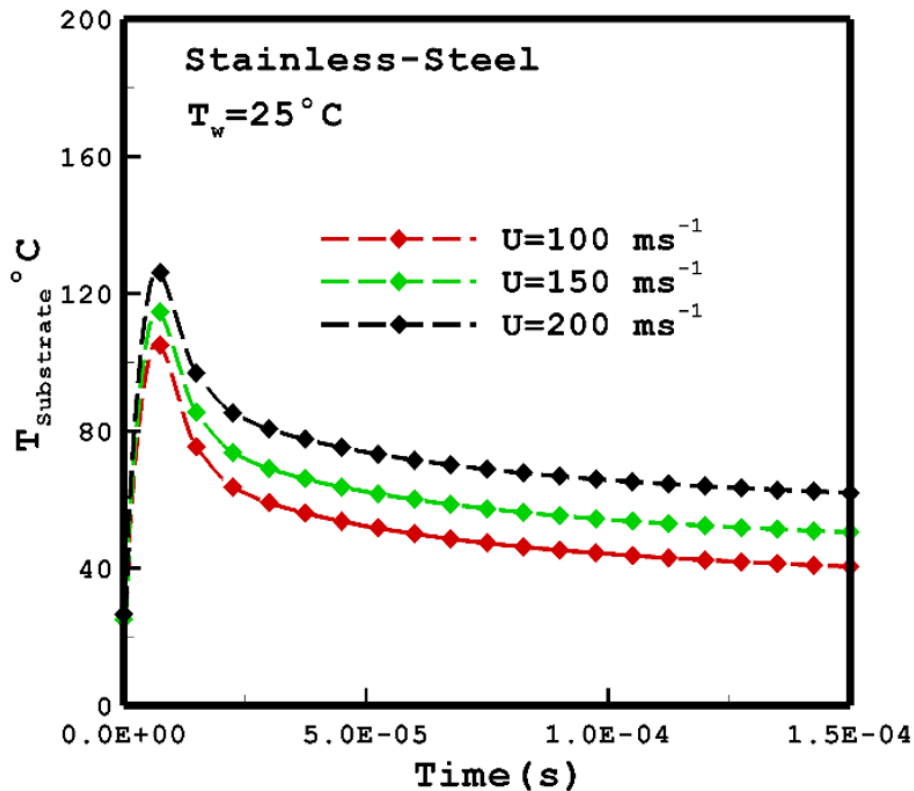


Figure 12. A stainless-steel substrate's temperature changes over time when aluminum droplets strike it at different speeds, $T_w = 25^\circ\text{C}$.

Due to the crucial roles that specific heat and thermal conductivity play in the dissipation of energy from the droplet, Figure 13 emphasizes the impact of substrate grade on heat transfer. Copper, being more thermally conductive than stainless steel and nickel, promotes faster cooling. This observation is supported by Fig. 14, which illustrates the dependence of thermal energy dissipation on the material's conductivity. Finally, Fig. 15 presents the temperature contours over time for the different substrate grades.

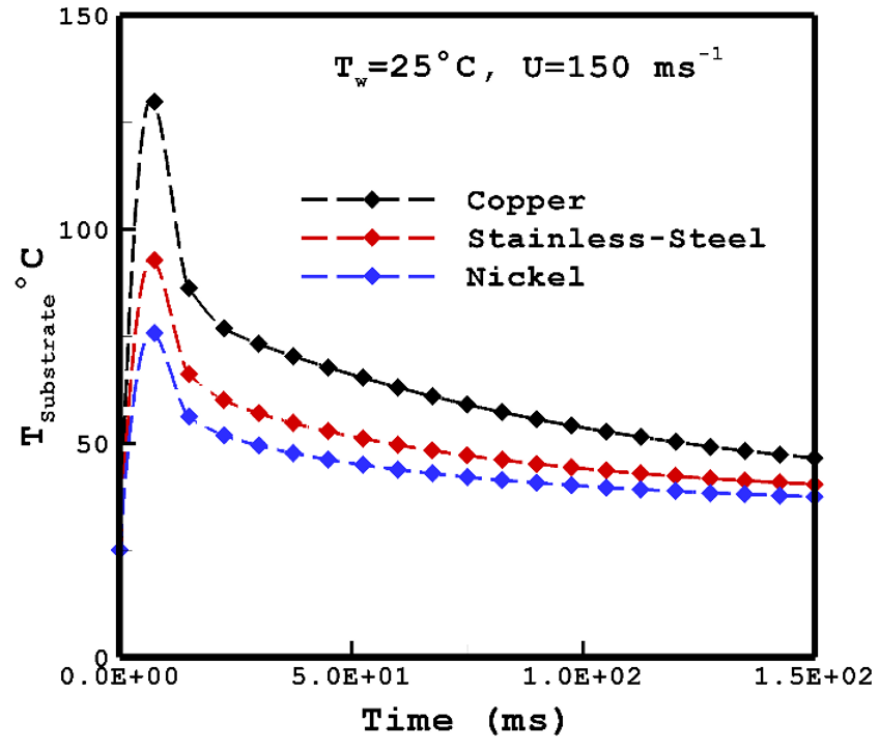


Figure 13. Temporal evolutions of the temperature of substrates of different grades subjected to aluminum droplet impact.

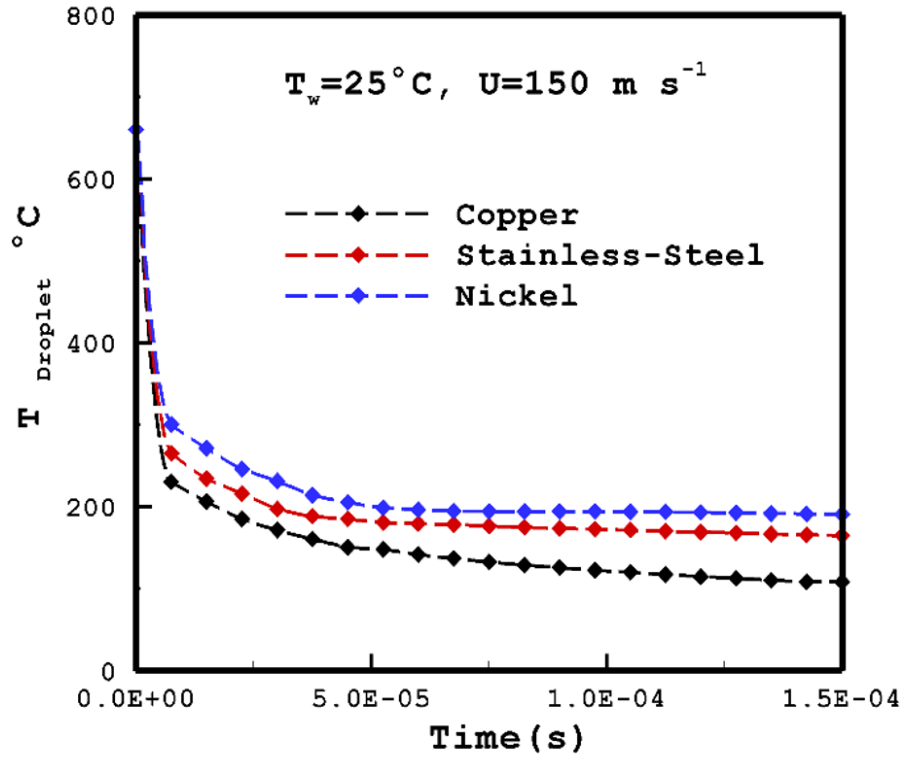
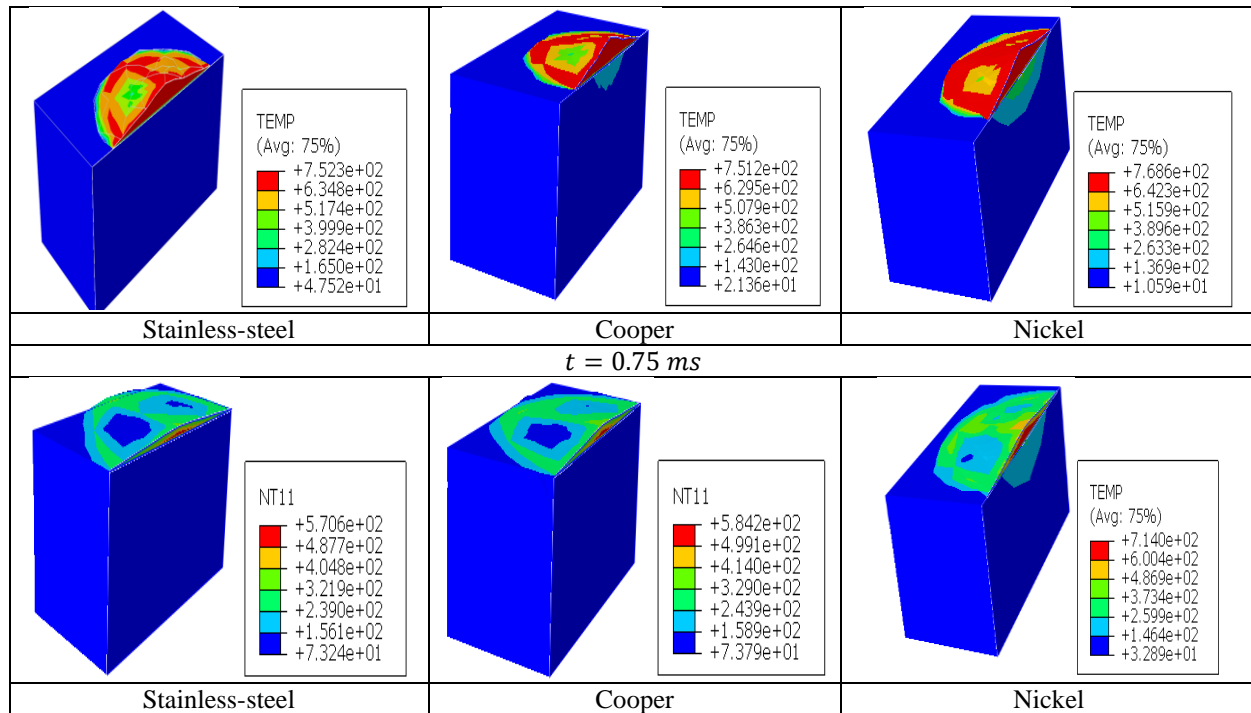


Figure 14. Temporal evolution of the temperature of an aluminum droplet impacting various substrate materials ($U = 150\text{ ms}^{-1}, T_w = 25^\circ\text{C}$).



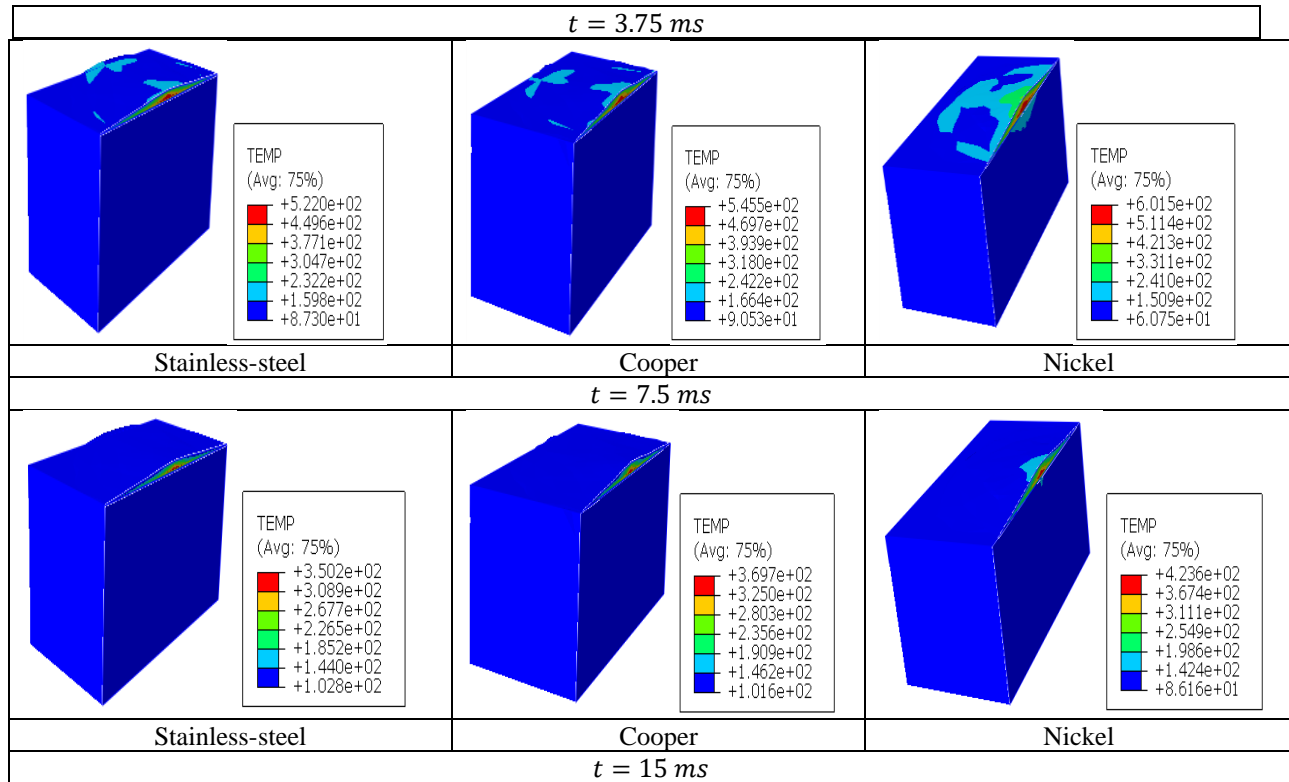


Figure 15.

Temporal evolutions of the temperature of an aluminum droplet impacting various substrate materials ($U = 150 \text{ ms}^{-1}$, $T_w = 25 \text{ }^\circ\text{C}$).

Figure 16 shows that the thickness of the solidified zone of the droplet evolves in a non-significant manner over time, regardless of the initial substrate temperature. This influence remains limited, as the temperature is below the melting point of the droplet's base metal. In contrast, the metallurgical nature of the substrate, namely its grade, has a more pronounced effect on the solidification thickness, as observed in Fig. 17.

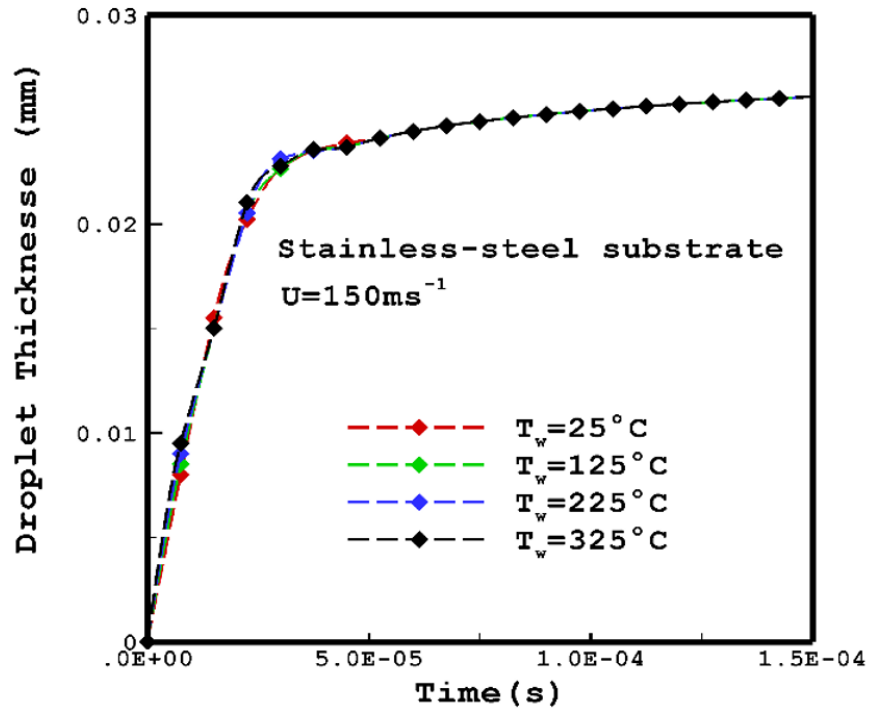


Figure 16. Evolution of the solidification thickness of an Aluminum droplet on a stainless-steel substrate at variable temperatures.

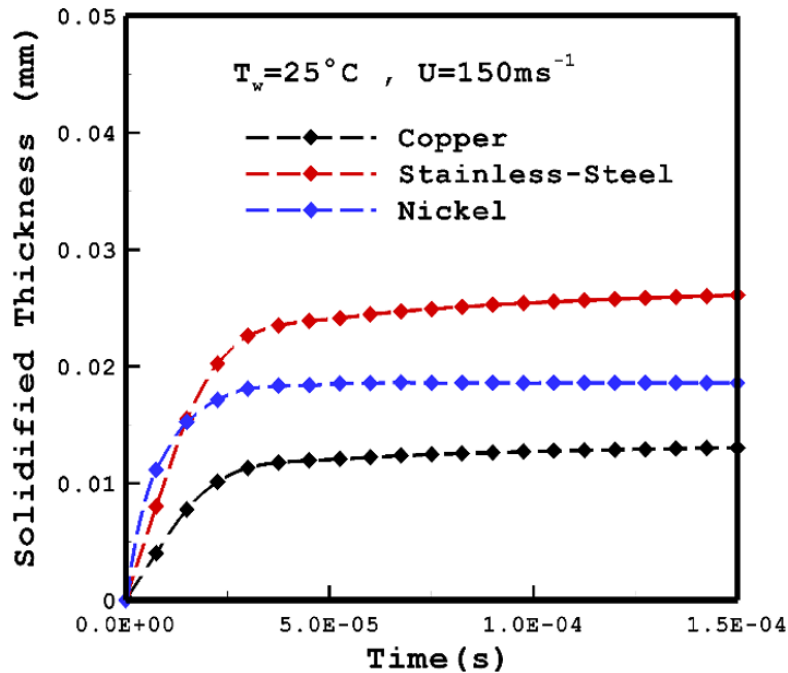


Figure 17. Evolution of the solidification thickness of an Aluminum droplet on Substrates of varying grades.

4.2. A Multiparticle System

In order to gain a deeper understanding of the phenomenon, a study was conducted on the successive impact of three superimposed particles to analyze their flattening behavior and the associated heat transfer mechanisms. The results are presented in Figures 18 and 19.

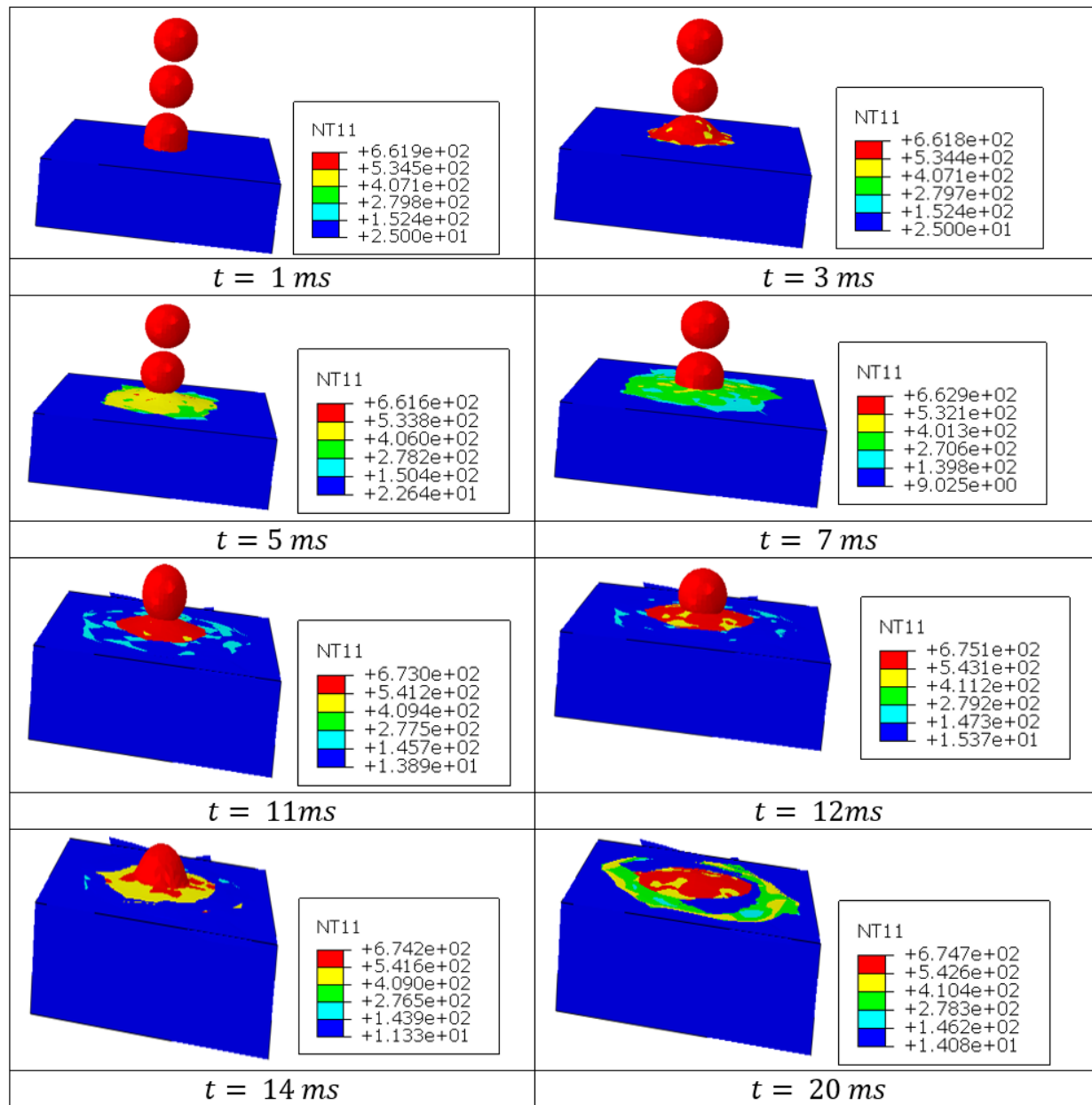


Figure 18. Temperature contour distribution for various substrate grades.

Figure 18 illustrates the temperature contours over time during the impact, and finally, Fig. 19 illustrates the solidification process of the three sequentially deposited particles. The first comes into

direct contact with the substrate surface, the second rests on the flattened surface of the first, and the third follows the same pattern. The substrate temperature varies with each impact.

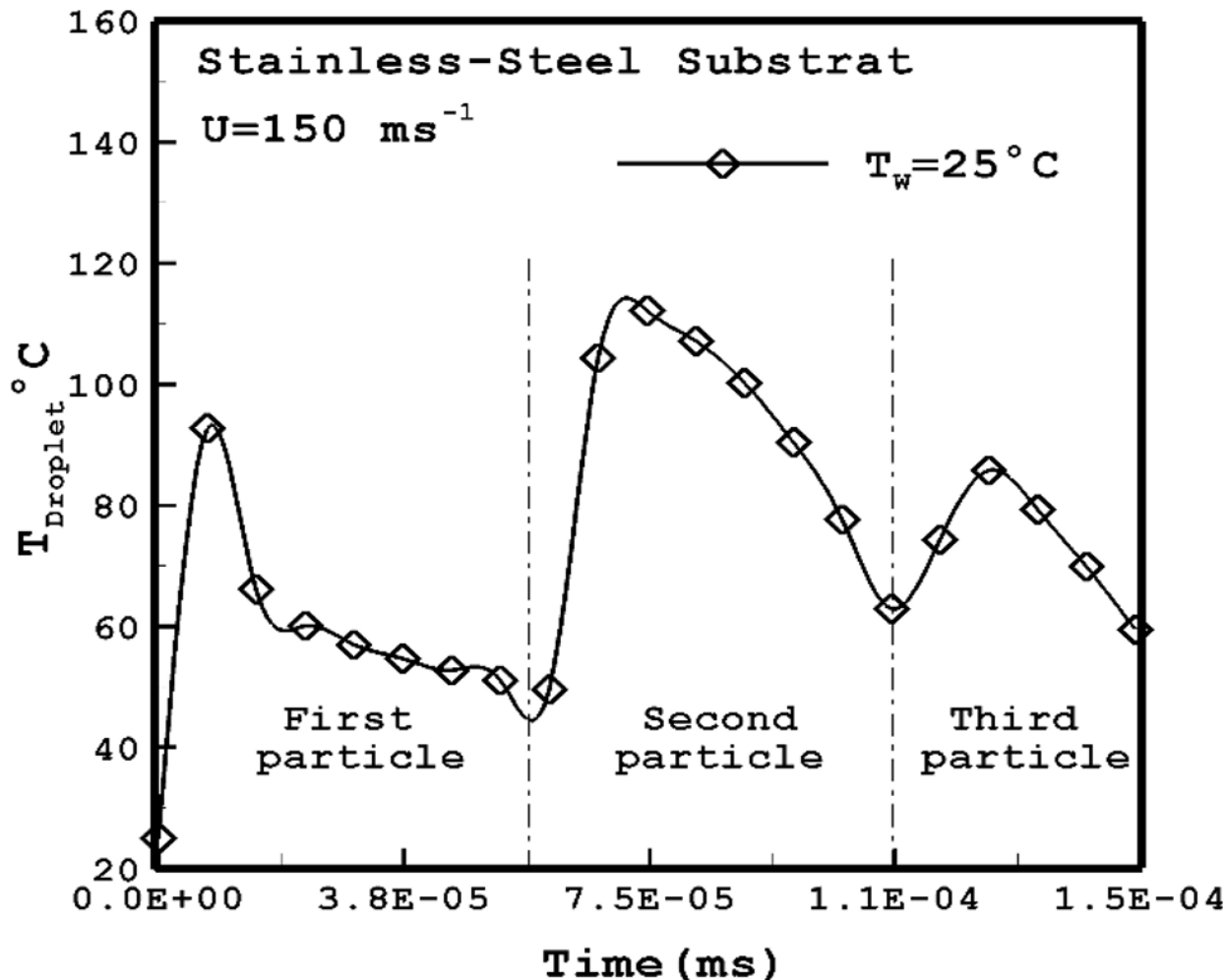


Figure 19. Temporal variation of substrate temperature during the impact of three particles.

5. Conclusion

In this work, the deformation and spreading of a single aluminum droplet were simulated to represent the thermal spraying process. Instead of treating the particle as a weakly bonded solid, a coupled thermo-mechanical framework was applied, in which the droplet was modeled as a fluid. The governing equations were solved using ABAQUS/Explicit, enabling detailed analysis of the impact dynamics. The key findings of this simulation can be summarized as follows:

- The viscous characteristics of molten aluminum are found to be suitable for modeling this kind of issue.
- Considering temperature-dependent material properties is a relevant approach for modeling this type of phenomenon.
- The introduction of a variable thermal contact conductance significantly influences the mechanisms of lamella (splat) formation as well as the thermal transfer phenomena.

- The impact dynamics, particularly the particle velocity, govern the effectiveness of adhesion and the morphology of the resulting deposit.
- Tribological interactions, particularly the coefficient of friction, contribute to energy dissipation mechanisms and particle anchoring.
- The surface roughness and compatibility of the particle and substrate alloys, as well as other properties of the materials themselves, are significant to the quality of the coating in the end.
- Both experimental data and prior simulations corroborate the outcomes of the suggested model. Thus, this model could be taken into account for future research into how substrate surface conditions, droplet size, and number affect the lamella formation mechanism.

Transparency:

The authors confirm that the manuscript is an honest, accurate, and transparent account of the study; that no vital features of the study have been omitted; and that any discrepancies from the study as planned have been explained. This study followed all ethical practices during writing.

Copyright:

© 2025 by the authors. This article is an open-access article distributed under the terms and conditions of the Creative Commons Attribution (CC BY) license (<https://creativecommons.org/licenses/by/4.0/>).

References

- [1] W. Liu, G. Wang, and E. Matthys, "Thermal analysis and measurements for a molten metal drop impacting on a substrate: Cooling, solidification and heat transfer coefficient," *International Journal of Heat and Mass Transfer*, vol. 38, no. 8, pp. 1387-1395, 1995. [https://doi.org/10.1016/0017-9310\(94\)00262-T](https://doi.org/10.1016/0017-9310(94)00262-T)
- [2] K. K. Subedi and S.-C. Kong, "Particle-based approach for modeling phase change and drop/wall impact at thermal spray conditions," *International Journal of Multiphase Flow*, vol. 165, p. 104472, 2023. <https://doi.org/10.1016/j.ijmultiphaseflow.2023.104472>
- [3] M. Pasandideh-Fard, R. Bhola, S. Chandra, and J. Mostaghimi, "Deposition of tin droplets on a steel plate: simulations and experiments," *International Journal of Heat and Mass Transfer*, vol. 41, no. 19, pp. 2929-2945, 1998. [https://doi.org/10.1016/S0017-9310\(98\)00023-4](https://doi.org/10.1016/S0017-9310(98)00023-4)
- [4] S. Attari *et al.*, "Thermo-mechanical modeling and simulation of impact and solidification of an aluminum particle," *Mathematical Modelling of Engineering Problems*, vol. 10, no. 2, p. 389-397, 2023.
- [5] S. D. Aziz and S. Chandra, "Impact, recoil and splashing of molten metal droplets," *International Journal of Heat and Mass Transfer*, vol. 43, no. 16, pp. 2841-2857, 2000. [https://doi.org/10.1016/S0017-9310\(99\)00350-6](https://doi.org/10.1016/S0017-9310(99)00350-6)
- [6] G. Trapaga, E. Matthys, J. Valencia, and J. Szekely, "Fluid flow, heat transfer, and solidification of molten metal droplets impinging on substrates: comparison of numerical and experimental results," *Metallurgical Transactions B*, vol. 23, no. 6, pp. 701-718, 1992. <https://doi.org/10.1007/BF02656450>
- [7] D. Attinger, Z. Zhao, and D. Poulikakos, "An experimental study of molten microdroplet surface deposition and solidification: Transient behavior and wetting angle dynamics," *Journal of Heat Transfer*, vol. 122, no. 3, pp. 544-556, 2000. <https://doi.org/10.1115/1.1287587>
- [8] M. V. Gielen, R. de Ruiter, R. B. Koldeweij, D. Lohse, J. H. Snoeijer, and H. Gelderblom, "Solidification of liquid metal drops during impact," *Journal of Fluid Mechanics*, Vol. 883, p. A32, 2020. <https://doi.org/10.1017/jfm.2019.886>
- [9] Y. Zhang, S. Matthews, and M. Hyland, "Role of solidification in the formation of plasma sprayed nickel splats through simulation and experimental observation," *International Journal of Heat and Mass Transfer*, vol. 115, pp. 488-501, 2017. <https://doi.org/10.1016/j.ijheatmasstransfer.2017.07.072>
- [10] E. Dalir, A. Dolatabadi, and J. Mostaghimi, "Modeling the effect of droplet shape and solid concentration on the suspension plasma spraying," *International Journal of Heat and Mass Transfer*, vol. 161, p. 120317, 2020. <https://doi.org/10.1016/j.ijheatmasstransfer.2020.120317>
- [11] N. Zeoli, S. Gu, and S. Kamnis, "RETRACTED: Numerical modelling of metal droplet cooling and solidification," *International Journal of Heat and Mass Transfer*, vol. 51, no. 15, pp. 4121-4131, 2008. <https://doi.org/10.1016/j.ijheatmasstransfer.2007.11.044>
- [12] P. Grant, B. Cantor, and L. Katgerman, "Modelling of droplet dynamic and thermal histories during spray forming—II. Effect of process parameters," *Acta metallurgica et materialia*, vol. 41, no. 11, pp. 3109-3118, 1993. [https://doi.org/10.1016/0956-7151\(93\)90040-Y](https://doi.org/10.1016/0956-7151(93)90040-Y)

- [13] S. Alavi and M. Passandideh-Fard, "The effects of thermal shrinkage on coating formation in thermal spray processes: A numerical approach," in *Proceedings of the 18th Annual International Conference on Mechanical Engineering (ISME 2010)* (pp. 11–13). Sharif University of Technology, Tehran, Iran, 2010.
- [14] J. F. Sánchez-Pérez, G. Jorde-Cerezo, A. Fernández-Roiz, and J. A. Moreno-Nicolás, "Mathematical modeling and analysis using nondimensionalization technique of the solidification of a splat of variable section," *Mathematics*, vol. 11, no. 14, p. 3174, 2023. <https://doi.org/10.3390/math11143174>
- [15] J. Xie, D. Nélias, H. Walter-Le Berre, K. Ogawa, and Y. Ichikawa, "Simulation of the cold spray particle deposition process," *Journal of Tribology*, vol. 137, no. 4, p. 041101, 2015. <https://doi.org/10.1115/1.4030257>
- [16] M. Xue, Y. Heichal, S. Chandra, and J. Mostaghimi, "Modeling the impact of a molten metal droplet on a solid surface using variable interfacial thermal contact resistance," *Journal of Materials Science*, vol. 42, no. 1, pp. 9–18, 2007. <https://doi.org/10.1007/s10853-006-1129-x>
- [17] Y. Liao, Y. Zheng, Z. Zheng, and Q. Li, "Numerical simulation of zirconia splat formation and cooling during plasma spray deposition," *Applied Physics A*, vol. 122, p. 654, 2016. <https://doi.org/10.1007/s00339-016-0192-7>
- [18] L. Suli, W. Zhengying, D. Jun, W. Pei, and L. Bingheng, "A numerical analysis on the metal droplets impacting and spreading out on the substrate," *Rare Metal Materials and Engineering*, vol. 46, no. 4, pp. 893–898, 2017. [https://doi.org/10.1016/S1875-5372\(17\)30118-2](https://doi.org/10.1016/S1875-5372(17)30118-2)
- [19] S. Danouni, A. A. El-hadj, M. Zirari, and M. Belharizi, "A thermo-mechanical analysis of a particle impact during thermal spraying," *Applied Surface Science*, vol. 371, pp. 213–223, 2016. <https://doi.org/10.1016/j.apsusc.2016.02.226>
- [20] Y. Zhao *et al.*, "Influence of substrate properties on the formation of suspension plasma sprayed coatings," *Journal of Thermal Spray Technology*, vol. 27, pp. 73–83, 2018. <https://doi.org/10.1007/s11666-017-0671-1>
- [21] C. Premaram, P. U. Gaur, A. P. Mobarsa, and K. Chaudhary, "Thermal spray coating applications in tribology: Recent case studies," *Journal of Thermal Spray and Engineering*, vol. 4, pp. 87–93, 2024.
- [22] Z. Tang *et al.*, "Influence of spray angle on particle deposition and thermal shock lifetime of embedded micro-agglomerated particle coatings," *Coatings*, vol. 14, no. 2, p. 199, 2024. <https://doi.org/10.3390/coatings14020199>
- [23] M. Zirari, A. A. El-Hadj, and N. Bacha, "Numerical analysis of partially molten splat during thermal spray process using the finite element method," *Applied Surface Science*, vol. 256, no. 11, pp. 3581–3585, 2010. <https://doi.org/10.1016/j.apsusc.2009.12.158>
- [24] M. Pasandideh-Fard and J. Mostaghimi, "On the spreading and solidification of molten particles in a plasma spray process effect of thermal contact resistance," *Plasma Chemistry and Plasma Processing*, vol. 16, no. Suppl 1, pp. S83–S98, 1995. <https://doi.org/10.1007/BF01512629>
- [25] S. Oukach, H. Hamdi, M. El Ganaoui, and B. Pateyron, "Thermal effects on the spreading and solidification of a micrometric molten particle impacting onto a rigid substrate," *Fluid Dynamics & Materials Processing*, vol. 8, no. 2, pp. 173–195, 2012.
- [26] A. Dinsdale and P. Queded, "The viscosity of aluminium and its alloys—A review of data and models," *Journal of Materials Science*, vol. 39, pp. 7221–7228, 2004. <https://doi.org/10.1023/B:JMSC.0000048735.50256.96>